Effects of interface state density on the carrier transport and performance of metal-insulator-semiconductor (MIS) type thin film solar cells

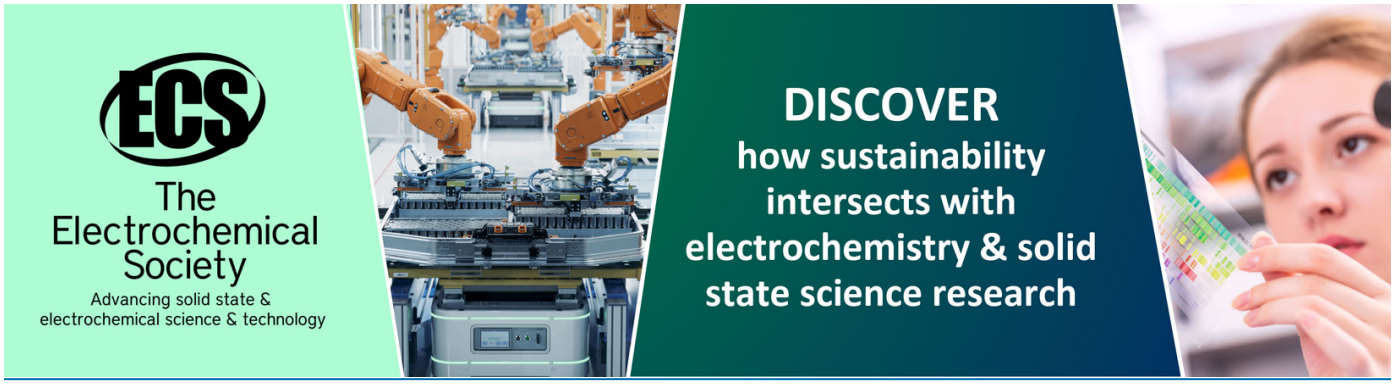

IOP Conf. Series: Journal of Physics: Conf. Series **1481** (2020) 012005 doi:10.1088/1742-6596/1481/1/012005

Effects of interface state density on the carrier transport and performance of metal-insulator-semiconductor (MIS) type thin film solar cells

Fandi Oktasendra[1*], Rahmat Hidayat[1] and Rizky Indra Utama[2]

[1] Department of Physics, Faculty of Mathematics and Natural Sciences, Universitas Negeri Padang, Jl. Prof. Dr. Hamka, Air Tawar, Padang 25131, Indonesia
[2] Department of Civil Engineering, Faculty of Engineering, Universitas Negeri Padang, Jl. Prof. Dr. Hamka, Air Tawar, Padang 25131, Indonesia

*f.oktasendra@fmipa.unp.ac.id

Abstract. Interface state density plays a significant role in determining the behaviour and characteristics of optoelectronic devices. In this paper, we investigated the effect of the interface state density on the carrier transport and performance in ZnO based-metal-instulator-semiconductor (MIS) type solar cells. Semi-analytical calculations were performed to obtain the solar cell's performance characteristics, i.e., the short circuit current, open-circuit voltage, fill-factor, and efficiency. Most possible carrier transport mechanisms including minority carrier diffusion, field emission (tunnelling) and carrier recombination were taken into account in investigating the role interface state density on the current profile. It was found that the effect of interface state density is dependent on the oxide thickness. At thicknesses higher than the critical thickness of the oxide layer the increase of the density of states causes the performance of the solar cells to drop.

1. Introduction

Metal-insulator-semiconductor (MIS) type solar cells have attracted a lot of interest in the search for low cost photovoltaic solar energy conversion. Compared to p-n junction solar cells, they are relatively easy to fabricate and much cheaper for large scale production [1-4]. The introduction of insulating layer between the metal and semiconductor has been proven to be able to improve the performance characteristics of the solar cells. In the last decades, the development of MIS type solar cells has considerably much progressed, such as the use of transparent conductive oxides (TCO) to replace metals that have low transparencies [5 -8]. TCO are basically semiconductors with wide band gap thus are mainly used as front contact allowing the incident light to penetrate into the substrate layer without losing much energy due to absorption [9]. TCO usually used in MIS structures are indium tin oxide (ITO), SnO_2, TiO2, fluorine tin oxide (FTO) and ZnO [10-13]. Among these TCO, ZnO and ITO have the major advantage for their low-cost fabrication process and low-temperature needed for deposition[14]. However, ZnO has more superiority for its excellence property to enhance the light trapping effect owing to its textured surface [15-16].

In MIS structures, the interface states or interface traps are always present at or very close to the insulator/semiconductor interface containing an energy distribution within the band gap of the semiconductor. Previous experiments have shown that the existence of interface states influence the

MIS device behavior and degrade the electrical characteristics of the device [17]. However, to our knowledge, the impact of interface states on the MIS solar cells has not been fully understood.

The objective of the present work is to investigate analytically the effect of interface state density on the carrier transport and performance characteristics of a ZnO-based MIS type solar cell. We use some simple semi-analytical calculation to obtain the cell characteristics such as the short-circuit current, the open-circuit voltage and the power conversion efficiency.

2. Theoretical formulation

In this work, the ZnO based-MIS type solar cell analyzed is illustrated in Fig. 1. Wide band-gap ZnO acts as a window for incoming light replacing the metal electrode. Although ZnO is actually a semiconductor, but due to its wide band gap it behaves similarly to a metal with a Fermi energy lies closely above the conduction band. The SiO2 layer is assumed to be very thin (less than 2 nm), which is used to increase the Schottky barriers. The n-type doped silicon substrate performs as the absorber layer.

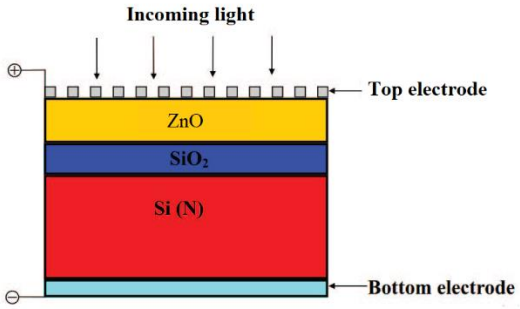

Figure 1. Schematically illustration of ZnO-based MIS type solar cell

The energy band diagram of ZnO-based MIS type solar cell in equilibrium condition and under illumination is shown in Figure 2. The diagrams show some parameters including ZnO work function (Φ_M), the electron affinity of silicon (χ), the interfacial layer potential (Δ) resulted from the difference between Φ_M and χ in the equilibrium condition, the interface state density (D_{it}), the surface state density at silicon (Q_{ss}), the potential barrier between ZnO and silicon (ϕ_{Bn0}) which is affected by the ZnO work function and interface states, the neutral energy level at interface states ($q\phi_0$), the built-in potential at silicon (ψ_{Bi}), the energy difference between conduction band edge and Fermi level at silicon (ϕ_n), the SiO2 layer width (δ), the depletion width (W_D), the energy gap of ZnO and silicon (E_{gZnO} and E_{gSi}, respectively) and the potential drop across the SiO_2 layer (V_i) and silicon (V_S), respectively. In equilibrium condition, the band bending in silicon layer is caused by the difference between the ZnO metal function and the electron affinity. This bending is further modified by the presence of surface charges at SiO2 and/or interface states, and the density of states at the interface change. At the interface, it can be found the acceptor interface trap (because Fermi level lies above ϕ_0) with the density D_{it} states/cm^2-eV having a constant value across the energy range from $q\phi_0 + E_V$ up to the Fermi level. Thus the charge density at the silicon surface, Q_{ss} is given by [19]

$$Q_{ss} = -qD_{it}\left(E_g - q\phi_0 - q\phi_{Bn0}\right). \quad \text{C/cm}^2 \quad (1)$$

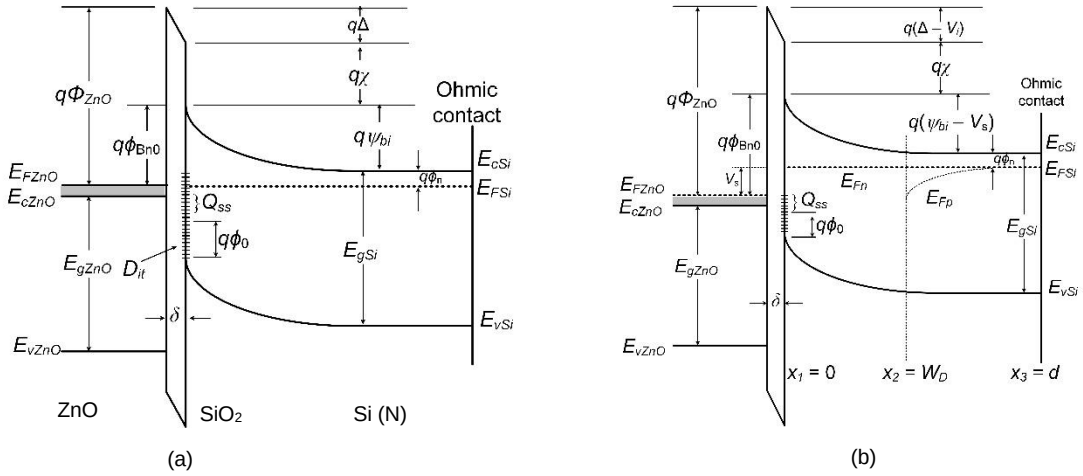

Figure 2. Energy band diagrams of proposed ZnO-based MIS type solar cell (a) in equilibrium condition and (b) under illumination. (Adopted from Ref [18])

Under illuminated condition, the potential drop V_s appears in the silicon layer causing the height of Schottky barriers to be lower by $\psi_{Bi} - V_s$. In addition, V_s also affects the depletion width through [19]

$$W_d = \sqrt{\frac{2\varepsilon_s}{qN_D}\left(\phi_{bi} - V_s - k_B T / q\right)}. \quad (2)$$

Furthermore, the surface charge is modified due to the potential drop because of the change of Schottky barriers by

$$Q_{ss} = -qD_{it}\left(E_g - q\phi_0 - q\left(\psi_{bi} - V_s\right) - q\phi_n\right). \quad (3)$$

Illumination also develops a voltage across the SiO2 layer, denoted as V_i, causing the alteration of the interfacial layer potential by $\Delta - V_i$ (See Fig. 1 (b)). If the space charge at the silicon is ignored, this potential drop is given by

$$\Delta - V_i = -\frac{\delta Q_{ss}}{\varepsilon_i}, \quad (4)$$

where ε_i is the permittivity of SiO2. Therefore, the voltage developed during illumination is given by $V = V_s + V_i$. The appearance of this voltage allows the flow of carriers in the cell resulting the cell is in forward bias condition. When the interface states are in equilibrium condition with the silicon, V_s can be expressed as [19]

$$V_s = \gamma V - \frac{\gamma\delta}{\varepsilon_i}\sqrt{2\varepsilon_s qN_D}\left(\sqrt{\psi_{Bi}} - \sqrt{\psi_{Bi} - V_s}\right), \quad (5)$$

where

$$\gamma = \frac{1}{1 + \dfrac{q^2 D_{it}\delta}{\varepsilon_i}}. \quad (6)$$

Here, ε_s and N_D represent the permittivity and doping density of silicon, respectively.

The current flows in an illuminated solar cell is given by [20]

$$J_{total} = J_{light} - J_{dark}. \quad (7)$$

where J_{light} is the current generated under by photon-electron interaction under illumination and J_{dark} is the current under bias condition. In the MIS-type solar cells, the photogenerated current is mainly created in the neutral region of the silicon J_{pw} and in the depletion region J_{dl}, which is strongly dependent of the wavelength of the incident photons, given by [18,20]

$$J_{light} = \int_{\lambda_{\min}}^{\lambda_g} \left[J_{dl}(\lambda) + J_{pw}(\lambda) \right] d\lambda. \quad (8)$$

where λ_{min} is the minimum wavelength of the solar spectrum, and λ_g is the wavelength corresponding to the silicon bandgap. For a monochromatic light, J_{dl} can be calculated by integrating the generation rate across the depletion region for a particular wavelength. Generation rate depends on the absorption coefficient of the silicon and the flux density of the solar spectrum. Since the ZnO has a high transparency owing to its wide band gap, the reflection rate at the top surface of the solar cell can be ignored. J_{pw} is mainly contributed by hole diffusion in the neutral region and can be calculated by solving the hole continuity equation at the depletion region boundary. Beside the contribution of J_{dl} and J_{pw}, the photocurrent can also be contributed by inverted holes at the semiconductor surface that quantum mechanically pass through the SiO2 potential barrier by tunnelling process from silicon into ZnO [5]. The dark current is dominated by three possible transport mechanisms, namely, the tunnelling current of the majority carriers (electrons), the minority carriers (holes) diffusion and the recombination of carriers (electron-hole pairs) [18, 19]. Previous report [18,21] showed that the tunnelling current is dominant under high bias voltage while minority carrier diffusion and carrier recombination dominate the dark current when the cell is moderately and lowly biased, respectively.

The performance parameters of the MIS-type solar cells can be deduced from the *I-V* characteristic curve, given by

$$I = I_{sc} - \sum_j I_{jo} \left[\exp\left(\beta_j V\right) - 1 \right], \quad (9)$$

where $\beta_j = q/(n_j kT)$ and Σ_j is a summation of the dark saturation currents. I_{sc} is called the short-circuit current defined as the current at which the voltage is zero. Open-circuit voltage V_{oc}, defined as the voltage at which the current is zero, is obtained from Eq. (9) by setting $I = 0$,

$$\sum_j I_{jo} \exp\left(\beta_j V_{OC}\right) = I_{sc} + \sum_j I_{jo}. \quad (10)$$

The power conversion efficiency can be expressed as

$$\eta = \frac{(FF) V_{OC} I_{SC}}{P_{in}}, \quad (11)$$

where P_{in} is the total input power and *FF* is called the Fill Factor, which is defined as

$$FF = \frac{I_m V_m}{I_{sc} V_{oc}} \quad (12)$$

where I_m and V_m represent the current and the voltage of the cells under maximum power condition. In this simulation, all parameters used in the computation are referred to Ref [18].

3. Result and Discussion

In this section the computation results of the ZnO-based MIS-type solar cells based on the theoretical model developed in this work are presented and analysed. Here, the main objective is to study the effect of interface state density D_{it} on the carrier transport and performance of the MIS-type solar cells. Figure 3 shows the effect of D_{it} on the short-circuit current J_{sc} that is plotted as a function of oxide thickness.

The values of D_{it} are varied in the same order from 1 to 5×10^{17} $m^{-2}eV^{-1}$. It can be seen that the J_{sc} drops drastically at lower SiO2 thickness as the D_{it} is increased. However, the value of J_{sc} remains constant at low oxide thicknesses. This can be explained as follows. It has been evident that increasing the oxide thickness until certain value (sometimes called as the critical thickness) can result in the decrease in short-circuit current, hence the efficiency of the solar cells (For further explanation, please read Ref [18]). When D_{it} increases, it will develop potential across the oxide layer resulting the increase of the barrier potential. As a consequence the tunneling current drops. Therefore, by increasing the interface state density, the abrupt decrease of short-circuit current becomes faster at lower oxide thicknesses. This finding suggests that the lower oxide thickness is favorable to get a constant short-circuit current. However, getting a very thin oxide thickness is challenging in fabrication wise. Therefore, one needs to find a limit of the oxide thickness above which the short-circuit current starts to drop.

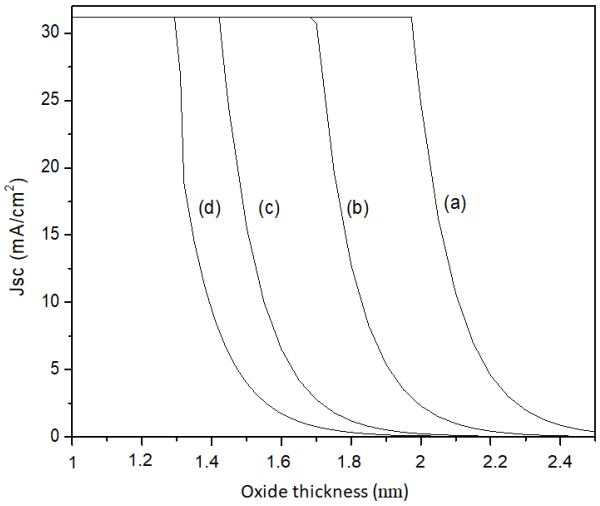

Figure 3. Short-circuit current J_{sc} as a function of SiO2 thickness of the ZnO-based MIS-type solar cells for different values of D_{it} (a) 1×10^{17} $m^{-2}eV^{-1}$, (b) $1{,}8 \times 10^{17}$ $m^{-2}eV^{-1}$, (c) $3{,}5 \times 10^{17}$ $m^{-2}eV^{-1}$, (d) 5×10^{17} $m^{-2}eV^{-1}$.

The same feature can be seen in the open-circuit voltage V_{oc} and the fill factor FF, as shown in Figure 4. Both V_{oc} and FF starts to drop after some certain value of oxide thickness, and increasing the D_{it} only to make the drop becomes faster at lower oxide thicknesses. However, the values of V_{oc} at lower oxide thickness slightly vary as the variation of D_{it}. This is different from the FF as it shows a constant value at lower oxide thickness akin to that of J_{sc}.

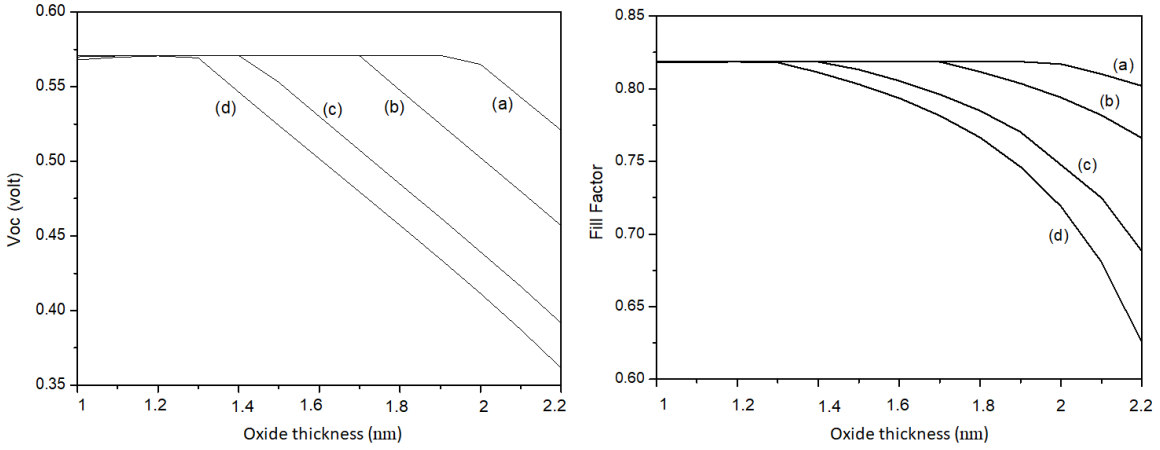

Figure 4. V_{oc} (left) and *FF* (right) as a function of SiO2 thickness of the ZnO-based MIS-type solar cells for different values of D_{it} (a) 1×10^{17} $m^{-2}eV^{-1}$, (b) $1{,}8 \times 10^{17}$ $m^{-2}eV^{-1}$, (c) $3{,}5 \times 10^{17}$ $m^{-2}eV^{-1}$, (d) 5×10^{17} $m^{-2}eV^{-1}$.

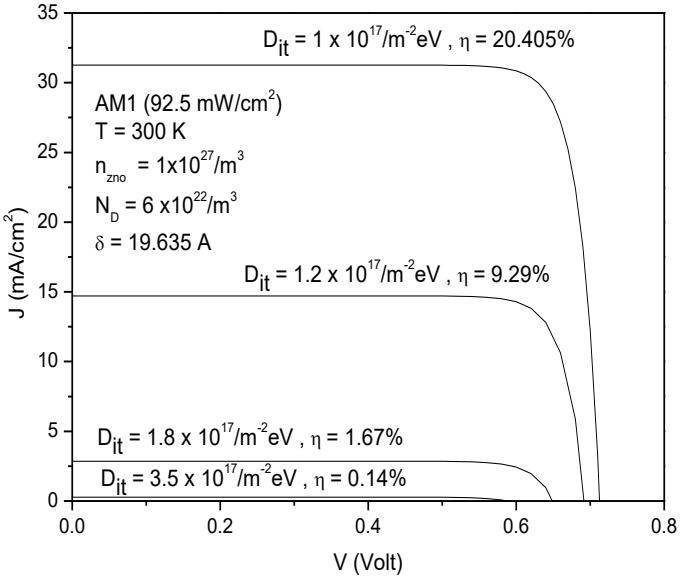

Figure 5. I-V characteristic curve of the ZnO-based MIS-type solar cells for different values of D_{it} (a) 1×10^{17} $m^{-2}eV^{-1}$, (b) 1.2×10^{17} $m^{-2}eV^{-1}$, (c) 1.8×10^{17} $m^{-2}eV^{-1}$, (d) 3.5×10^{17} $m^{-2}eV^{-1}$.

Figure 5 shows the current-voltage relation for the ZnO-based MIS-type solar cells. In order to see the effect of the D_{it}, the oxide thickness is chosen to be 1.9 nm, at which other parameters such as the doping density in the silicon and the carrier concentration at ZnO become optimum. As it is implicitly suggested from J_{sc}, V_{oc} and *FF,* the efficiency of the solar cells decreases as the increase of D_{it}. From this curve, it can be clearly seen than the decrease of J_{sc} contributes dominantly to the efficiency of the cell compared to other parameters.

4. Conclusion

The effect of interface state density on the performance parameters of the ZnO-based MIS type solar cells were studied using simple theoretical approach and semi-analytical simulation. Simulation results show that the interface state density can give a significant impact on the performance parameters of the MIS type solar cells. It is shown that the effect of interface state density is dependent on the oxide thickness. At thicknesses higher than the critical thickness of the oxide layer the increase of the density of states causes the performance of the solar cells to drop. Therefore, it is suggested to reduce the density of states in order to get a higher performance MIS solar cell.

References

[1] Bakhshi S, Zin N, Ali H, et al. 2018 *Sol Energ Mat Sol C*. **185** 505–510.
[2] Chang TY, Chang CL, Lee HY, et al. 2010 *IEEE Electron Dev Lett.* **31(12)** 1419–1421.
[3] Garud S, Gampa N, Allen TG, et al. 2018 *Phys Status Solidi.* **215(7)** 1700826–1/6.
[4] Lee TD, Ebong AU. 2017 *Renew Sustain Energ Rev.* **70** 1286–1297.
[5] Wenas WW, Riyadi S. 2006 *Sol Energ Mat Sol C*. **22** 3261–3267.
[6] Pür FZ, Tataroğlu A. 2012 *Phys Scripta.* **86** 035802.
[7] Gao J, Kempa K, Giersig M, et al. 2016 *Adv Phys.* **65** 553–617.
[8] Cheknane A. 2009 *J Phys D Appl Phys.* **42** 115302.
[9] Hu YH, Xu HJ, Gao H, et al. 2011 *Mater Sci Forum.* **663** 1077–1080.

[10] Hocine D, Belkaïd MS, Lagha K. 2008 *Rev Energ Renew.* **11** 379–384.
[11] Thomas KRJ, Baheti A. 2013 *Mater Technol.* **28** 71–87.
[12] Kim C, Jo HJ, Kim DH, et al. 2012 *Mol Cryst Liq Cryst.* **565(1)** 52–58.
[13] Qin H, Liu HF, Yuan YZ. 2013 *Energ Mater.* **29** 70–76.
[14] Mishra A, Kumar A, Hodges D, et al. 2017 *Mater Technol.* **32** 829–837.
[15] Vadivel B, Sudha S, Gowrisankar P, et al. 2018 *Mater Technol.* **33(6)** 414–420.
[16] Zahirullah S, Prince J, Inbaraj FH. 2017 *Mater Technol.* **32** 755–763.
[17] Acar FZ, Buyukbas-Ulusan A, Tataroglu A. J. 2018 *Mater Sci.:Mater in Electron*.
[18] Noor FA, Oktasendra F, Sustini E, Khairurrijal K. 2018 *Mater Technol.* **33(14)** 865-871
[19] Shousha AHM. 1989 *Sol Wind Technol.* **6** 705–712.
[20] Card HC, Yang ES. 1976 *Appl Phys Lett.* **29** 51–53.
[21] Noor FA, Oktasendra F, Sustini E, Abdullah M, Khairurrijal K. 2013 *Mater Sci Forum*, **737** 1-8